

# ALMA Memo #270

## ALMA Configurations with complete UV coverage

David Woody  
Caltech, Owens Valley Radio Observatory, Big Pine, CA 93513

### Abstract

This memo discusses the importance of obtaining complete UV coverage for an interferometer array and presents configurations that achieve nearly complete coverage using earth rotation synthesis over a limited hour angle range. The configurations are symmetric circular arrays with S identical sectors. These configurations are shown to cover more than 90% of the UV-plane in a few hours for sources between  $-90^\circ$  and  $+50^\circ$  DEC for an array located at  $-23^\circ$  lat. The coverage surpasses 98% for sources at less than  $-10^\circ$  DEC or greater than  $+10^\circ$  DEC. The array diameter is approximately  $N^2 D / 4S$ , where N is the number of telescopes, D their diameter and S the degree of symmetry. An array of 63 twelve-meter telescopes in a five-fold symmetric circular configuration can provide complete UV coverage while achieving an angular resolution of better than .1 arcsec at 1 mm. This configuration will provide noise limited high accuracy images that are an excellent match to images from the Hubble telescope.

### I. Introduction

Radio interferometer arrays offer the option of tailoring the coverage in the Fourier plane (UV-plane) to optimize the performance for a particular type of observation. Unfortunately, there is no single optimum solution or class of solutions for all observations. ALMA will have configurations well suited to the types of projects we know will be done, such as the compact configuration for good surface brightness sensitivity and the 10-30 km diameter circular array for the maximum angular resolution. There should also be configurations in-between that work well for a large variety of observations. Many different configurations have been proposed with differing goals ranging from minimizing the “dirty” sidelobes [Kogan, 1999] to allowing for continuous scalability [Conway, 1999]. It has also been argued that the optimum configuration is one that gives uniform coverage within a given diameter circle in the UV-plane [Keto, 1997]. This memo advocates that beyond just uniform coverage at least one configuration should be dedicated to achieving nearly complete UV coverage with resolution as high as .1 arcsec at 1 mm.

A major part of astronomical research today requires observations across the whole spectrum. It is important that the various instruments used to obtain the observations have good fidelity and accuracy so that reliable comparison across the bands within an instrument and between entirely different spectral ranges can be made. This requires producing images that have been processed using a minimum number of assumptions about the astronomical field being imaged. At the high sensitivity levels achievable with ALMA many fields will have structure across the full primary beam. It can not even be assumed that all of the “real” features in an image are positive (i.e. the CMB anisotropy and SZ effect can produce negative flux relative to any observable reference in the sky).

The only way to ensure complete and accurate images with an interferometer array is to fully sample the full UV-plane. Most existing interferometer arrays do not have enough telescopes to fully sample the UV-plane while simultaneously achieving useful high angular resolution even with multiple configurations. ALMA, with upward of 60 antennas, will be the first interferometer capable of producing high-resolution images with nearly complete UV coverage in a single configuration. Such images would be the equivalent of a Hubble image and could be produced with a minimum of processing and no assumptions about the nature of the objects in the field. The images would be limited by the receiver noise and system calibration errors and not by missing UV data. Using improved amplitude [Bock et al., 1999] and phase calibration strategies [Carilli and Holdaway, 1999] the fidelity and accuracy of the images will enable a whole new class of projects requiring precise cross comparison of images. Several speakers at the Imaging99 conference in Tucson pointed out the importance of making accurate comparison between images.

It is important that at least one of the ALMA configurations be fully optimized for complete UV coverage. The only question is what the angular resolution will be for such a configuration and whether different configurations will be required for different declination ranges. The most compact configuration will provide complete UV coverage but at low angular resolution. This paper explores configurations that utilize earth rotation synthesis over a few hours to provide complete UV coverage at an interestingly high resolution and over the full declination range available to ALMA. The general approach is described in the following section while the detailed results are presented in section III. The issue of mosaicing large fields is discussed in the context of these high UV coverage configurations in section IV. Section V discusses the results of this study and a short conclusion is given in section VI.

## II. Idealized configurations

The first step in finding an “optimum” configuration is to define an objective metric to measure the performance of any particular configuration. The goal of this memo is to find array configurations that maximize the resolution while also giving nearly complete UV coverage. Earth rotation will be used to help fill in the UV-plane, but it is desirable to accomplish this with a minimum of observing time. The problem is further complicated by having to cover the full declination range available to ALMA, i.e.  $-90^\circ$  to  $+50^\circ$  DEC. It is particularly difficult to use earth rotation to fill in the UV-plane for sources near  $0^\circ$  DEC. A formal optimization procedure would involve assigning weights to these conflicting requirements and searching for configurations that maximize the overall performance.

This memo describes a simpler and less rigorous approach. The problem is tackled in two steps. The first step is to work on the idealized problem of finding the best configuration for an array at the South Pole observing polar sources. The second step is to place the configuration at the ALMA latitude, modify it by extending it in the North-South direction, and evaluating how well it performs over the full declination range.

We must now discuss what is meant by UV-coverage. A pair of antennas measures the UV visibility over the area given by the complex cross correlation of their aperture voltage patterns. This is a bell shaped spot of diameter  $2D$  where  $D$  is the

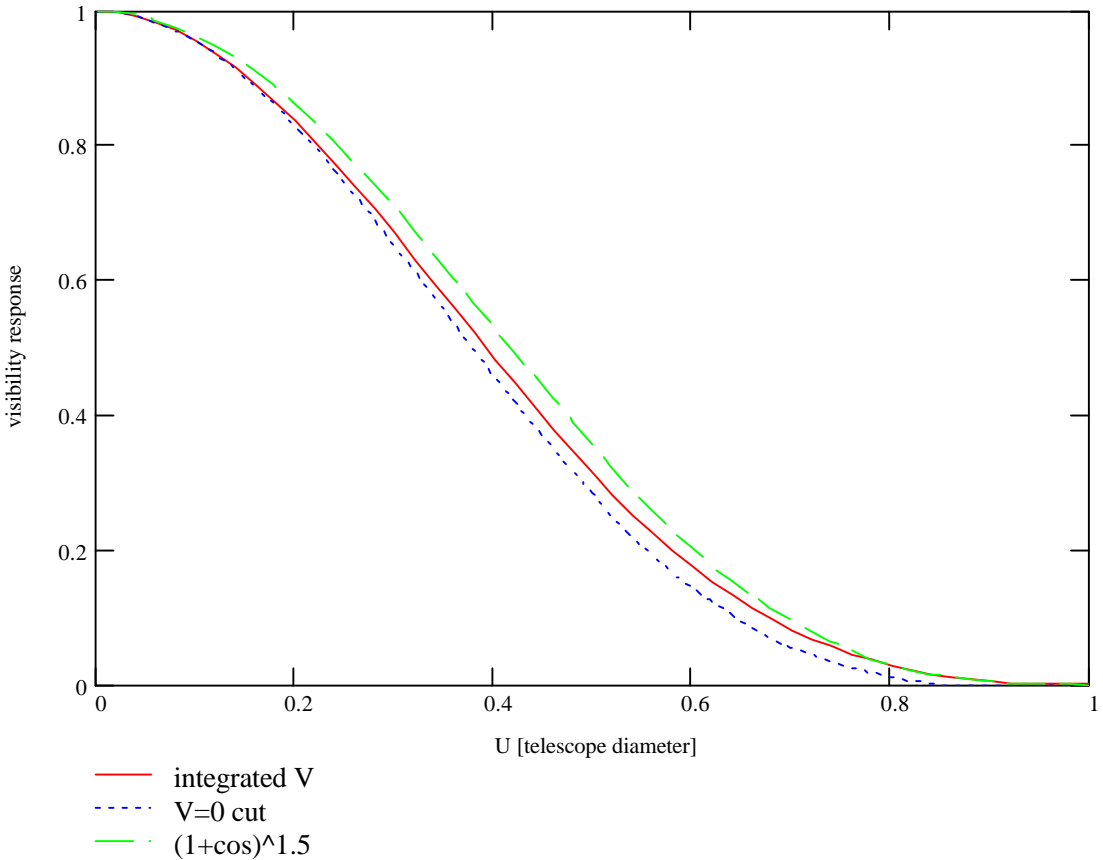


Fig. 1. Visibility response for  $-10$  dB Gaussian edge taper illumination pattern.

diameter of the antennas. Figure 1 shows the shape of the UV response function for a pair of antennas with Gaussian illumination and 10 dB edge taper. The response is closely approximated by  $((1+\cos(\pi r/D)/2)^{1.5}$ , which can be conveniently used for sensitivity estimates. The measured visibility for a single pointing of a pair of telescopes is the true visibility convolved with this response function. The visibilities on smaller UV scales can be reconstructed by measuring the visibilities at multiple pointings. This is known as mosaicing. Experience shows that you can reliably recover UV structure out to  $\sim D/2$  from the nominal UV point where the response drops to  $\sim 1/2$  of its peak value. Thus sampling the UV-plane so that no point on the plane is more than  $D/2$  from a nominal baseline point gives complete coverage of the UV-plane. Individual baselines sweep along ellipses as the earth rotates. A pair of elliptical tracks separated by  $D$  covers a swath of width  $2D$  across the UV-plane. Coarser sampling of the UV can be tolerated if the extent of the emission is much less than the primary beam. But with the sensitivity of ALMA, many fields will have detectable sources across the full primary beam and beyond. Note that the primary beam is less than 10 arcsec at the highest operating frequency for ALMA.

Starting with a source at  $-90^\circ$  DEC greatly simplifies the search for configurations because the baseline tracks become circles. A configuration with  $S$ -fold symmetry produces  $2S$  arcs for each unique baseline length. These arcs link together to form complete circles after only  $1/2S$  of a day. It is only necessary to find an  $S$ -fold

symmetric configuration that instantaneously covers all baseline lengths from 0 to the maximum baseline length with no gaps larger than D to achieve complete UV coverage. The vector orientation of the baselines does not matter since all baseline tracks become complete circles.

The initial approach to finding the requisite configuration was to try random placements of M antennas in a circle of diameter C to create a sub-array. The sub-array was rotationally duplicated S times to create an S-fold symmetric array of S×M antennas. The array was then tested to see how well it covered the baseline lengths from 0 to C. Repeated random sub-arrays were tried until a configuration with complete baseline length coverage was found. The array diameter C was then increased and another search for a satisfactory configuration was started. This continues until the array size, C, is so large that a configuration with complete coverage cannot be found. The failure to find a solution can be because all possible configurations have been tried and failed or you simply run out of computer time. Keto [1997] describes several more efficient methods for finding optimum configurations, but since the goal this memo is simply to show that high-resolution configurations with complete coverage exist, the algorithmically simpler random search approach is used.

The red triangles in fig. 2 show the results for up to six antennas in each sub-array of a five-fold symmetric configuration. The number of possible configurations increases dramatically as the number of antennas in the sub-array increases and it becomes impractical to use random guesses to cover the two dimensional array area. The optimal arrays distributed the antennas around the perimeter of the circle in a thin ring array very similar to the array configurations described by Eric Keto. This is reasonable since complete coverage is just an extension of the uniform coverage criterion used by Keto. For larger numbers of antennas the search was limited to purely circular arrays to reduce

Fig. 2. Array diameter (in units of the antenna diameter) vs. number of antennas for a five-fold symmetric circular array. The red triangles are for full 2-dim searches while the blue diamonds are for circular arrays.  $N^2/4S$  is plotted in purple.

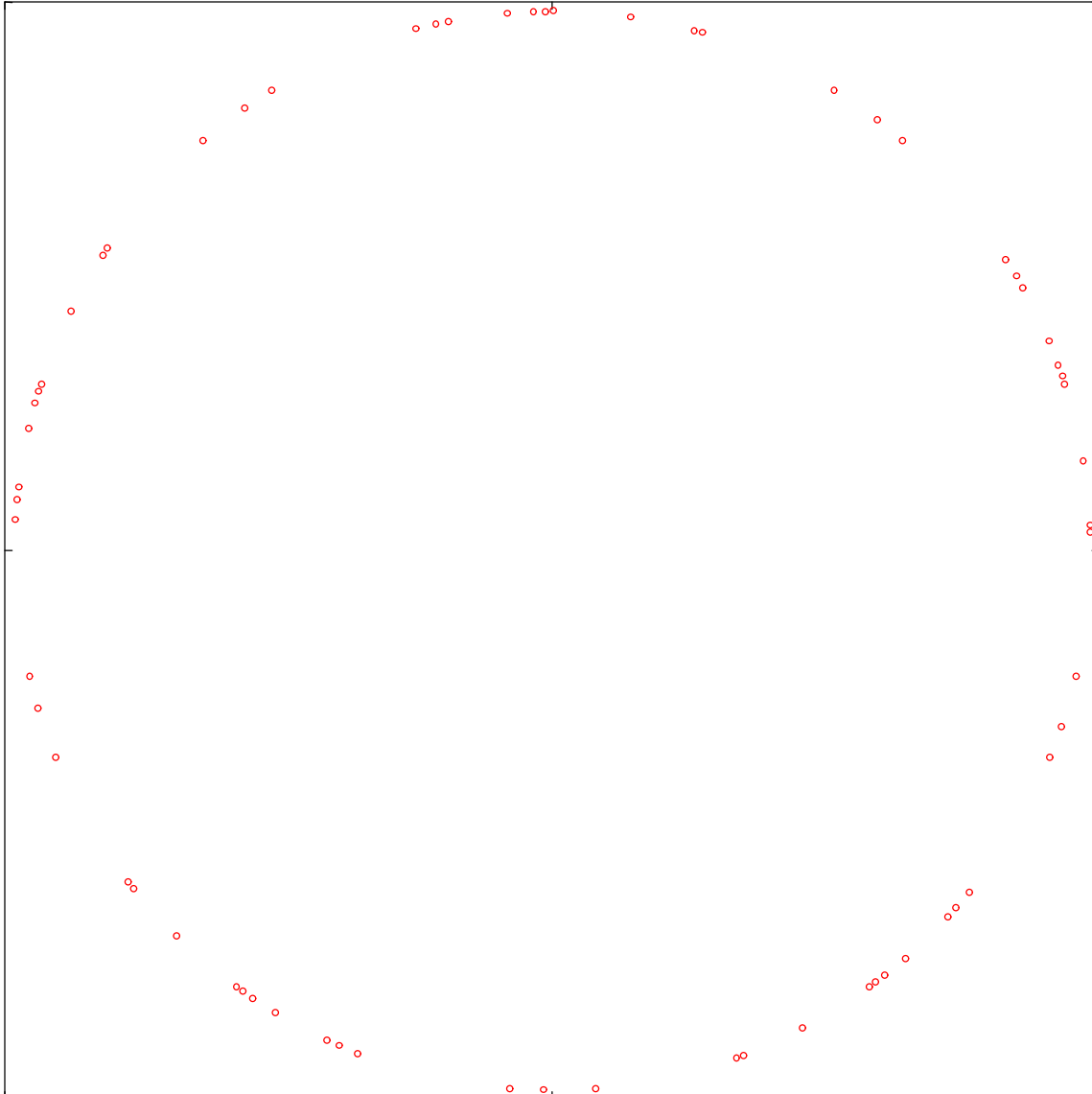


Fig. 3. Configuration for a five-fold symmetric circular array with 13 antennas in each sector. The antennas are 12 m diameter and the array diameter is 2 km.

the problem to a one-dimensional search. The results for five-fold symmetric circular configurations are plotted as blue diamonds in fig. 2. The curve  $N^2/4S$  ( $N$  is the total number of antennas and  $S$  is the symmetry order, five in this case) is also plotted in fig. 2 and corresponds to an average excess redundancy of a factor of two for the baseline length coverage. The deviation from this curve for the largest number of antennas is probably a result of not searching enough possible configurations even for the simpler circular arrays.

Figure 3 shows an example of a five-fold symmetric circular array with 13 antennas per sector. The instantaneous UV coverage for this configuration is shown in fig. 4. The signal-to-noise in each UV-cell is shown in fig. 5 as a function of the baseline length. The UV responsivity used for this plot corresponds to 12 m diameter telescopes with Gaussian illumination and -10 dB edge taper. The signal-to-noise is set by the total

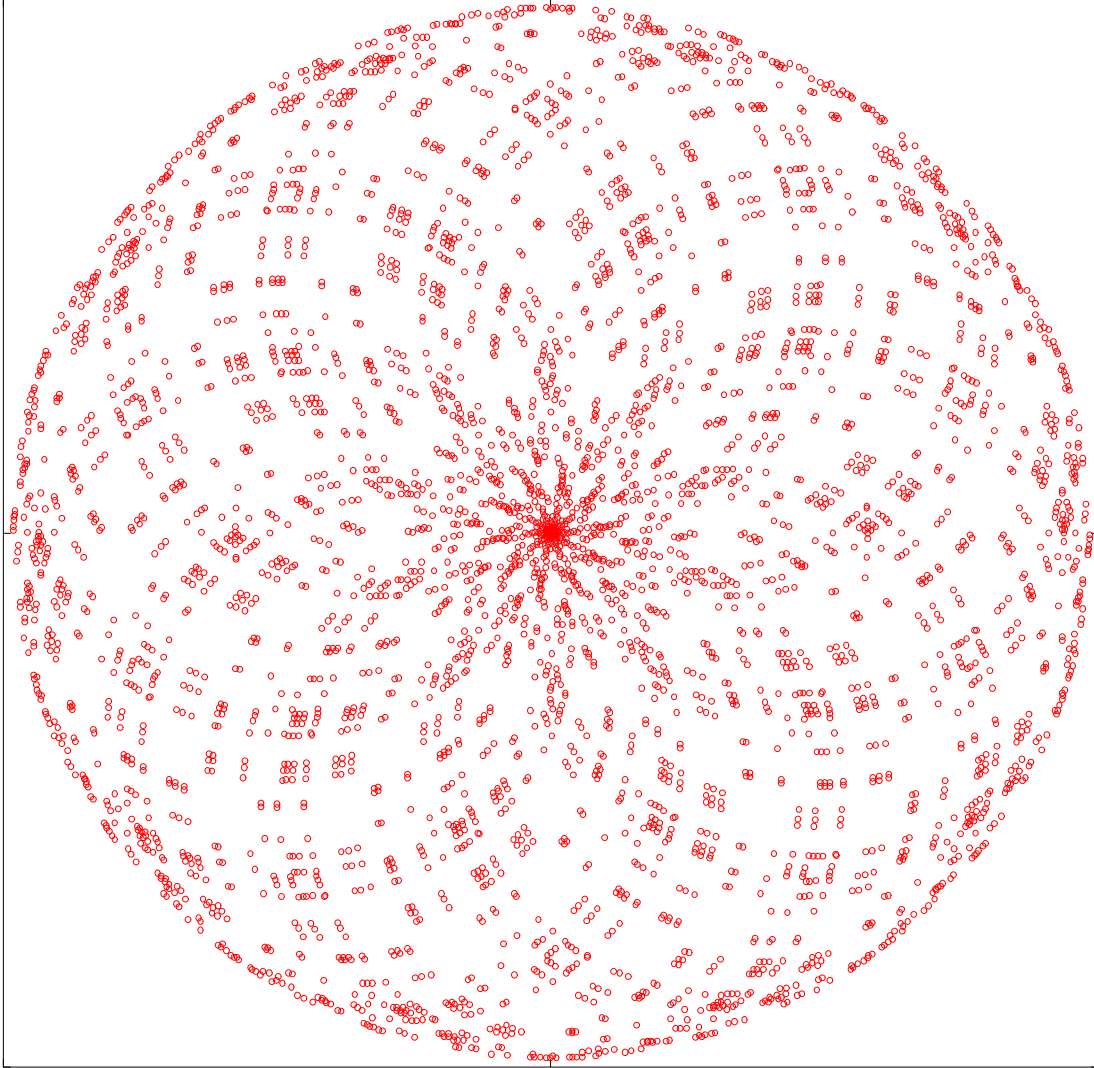


Fig. 4. Instantaneous UV coverage or the configuration in fig. 3. The diameter of the UV coverage is 4 km.

integration time per UV-cell. Redundant sampling and the rate at which earth rotation moves the UV coverage in the UV-plane is accounted for in the calculations. This radial distribution is typical of circular arrays. The large number of long baselines and the slow motion of the short baselines across the UV-plane accounts for the increased signal-to-noise for these baselines. The local variation in the signal-to-noise is only about a factor of two. A more uniform instantaneous coverage can probably be achieved using an S-sided constant diameter configuration [Keto, 1997], but since every UV-cell is covered by Earth rotation, the non-uniformity only weakly effects the signal-to-noise.

It remains to determine the UV coverage as a function of source declination and track duration once a circular configuration is found that has complete baseline length coverage. As will be shown in the next section these symmetric circular arrays do reasonably well over most of the declination range.

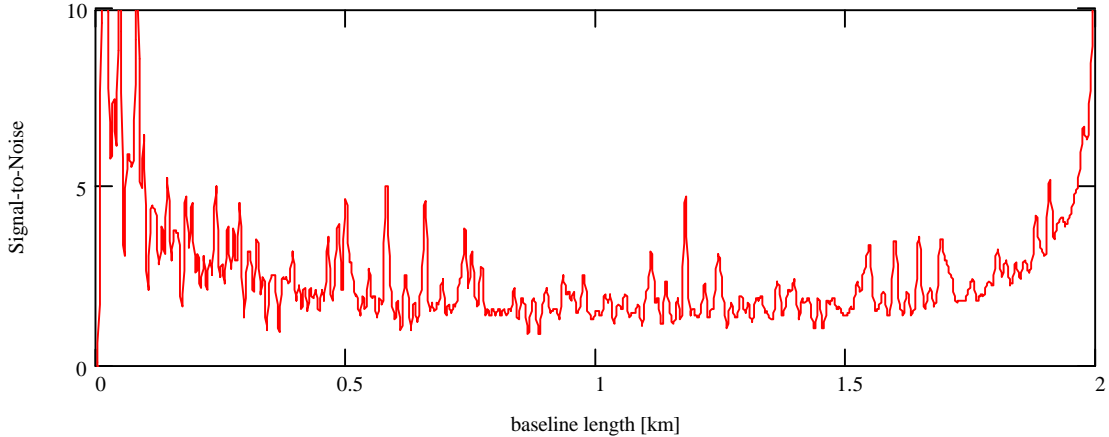


Fig. 5. Relative signal-to-noise in each UV-cell as a function of distance from the center of the UV-plane.

### III. ALMA array configuration study results

Configuration studies were done assuming that ALMA will have  $\sim 63$  antennas located at  $-23^\circ$  latitude. Symmetries of 63, 31, 21, 15, 13, 11, 9, 7, 5 & 3 with 1, 2, 3, 4, 5, 6, 7, 9, 13 & 21 antennas in each arc segment respectively were analyzed. The results are listed in Table I. The close packing limit for the antennas was handled by moving any pair of antennas separated by 1D so that they are separated by 1.2D before calculating the UV coverage.

The configuration search was based on a circular configuration when viewed from the pole, but the calculation of the UV coverage used the actual location of the array and the source declination. The algorithm included a north-south elongation ratio (east-west width held constant). An elongation of 1.5 in the north-south direction was chosen as a compromise between beam symmetry for polar sources and UV coverage for equatorial sources. Smaller elongation improves the UV coverage for equatorial sources but gives

Sym	Tele/sect.	Sect. Len [ant D]	Telescope positions [antenna diameters]	E-W width [km]
63	1	1.2	0	.29
31	2	3	0, 1.2	.36
21	3	6	0, 1.2, 4	.48
15	4	13	0, 1.2, 3, 9	.75
13	5	19	0, 1.2, 3, 10, 14	.94
11	6	27	0, 1.2, 5, 9, 15, 25	1.13
9	7	37	0, 1.2, 15, 21, 27, 29, 34	1.27
7	9	59	0, 1.2, 3, 9, 16, 29, 34, 44, 48	1.58
5	13	103	0, 1.2, 3, 7, 16, 18, 21, 45, 50, 58, 80, 81, 91	1.97
3	21	198	0, 1.2, 32, 35, 40, 41.2, 44, 47, 58, 74, 93, 96, 108, 109.2, 115, 119, 121, 143, 145, 172, 178	2.27

Table I. Configurations evaluated for ALMA. The E-W width assumes 12 m diameter antennas.

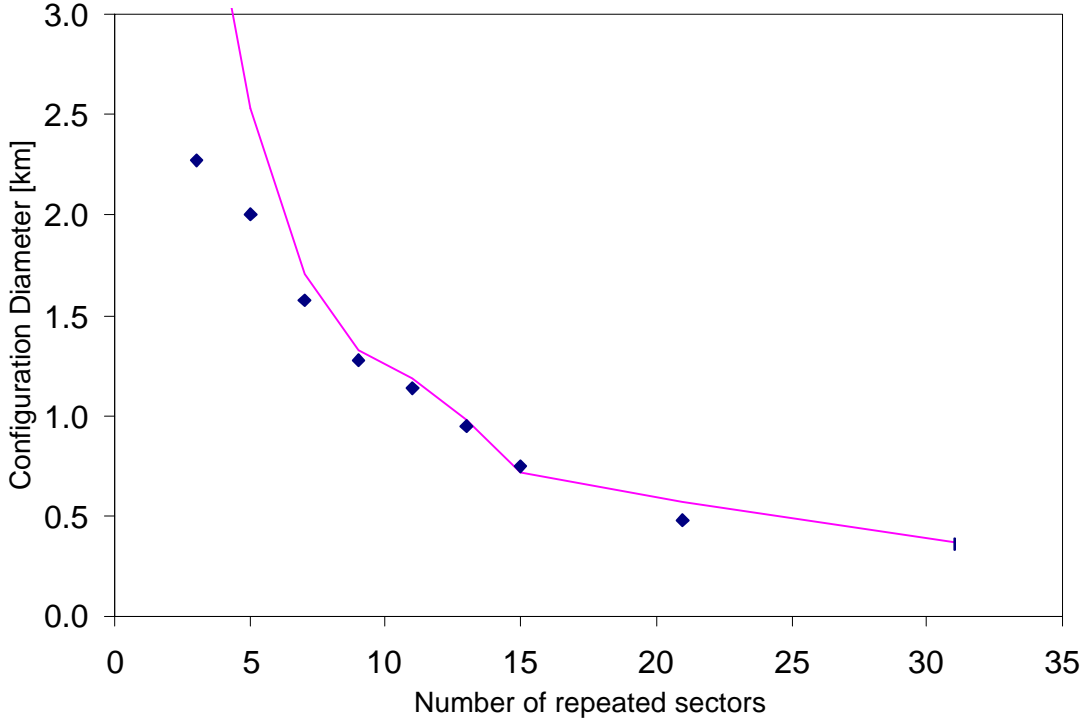


Fig. 6. ALMA configuration diameter as a function of the symmetry order for an array with  $\sim 63$  antennas.  $N^2 D / 4S$  is plotted in purple.

very asymmetric beams for polar sources.

The 63-fold symmetric array is the simplest case. It is simply a uniform circular array with a spacing of 1.2D between antennas. This configuration obviously has complete baseline length coverage and does not require any earth rotation to give complete UV coverage. Increasing the spacing would leave an unacceptable gap at baseline length  $\sim 1D$ . The 1.2D spacing already exceeds the 1D maximum gap requirement. This will be discussed further in the next section on the mosaicing.

The higher order symmetry configurations have only a few telescopes in each sector and all possible configurations were systematically tried. The number of telescopes in a sector and the sector length increase as the symmetry order decreases and it becomes impossible to try all possible arrangements of telescopes in a sector. Many random placements were tried to find successful configurations for these cases. The number of false guesses increases dramatically as you approach the maximum possible sector length providing complete baseline length coverage. Typically, the search for valid configurations at ever-longer sector lengths was halted when a million tries failed to find a successful configuration. This doesn't find the absolutely highest resolution circular configuration with complete baseline length coverage, but is probably within 20% of the maximum. Table I lists the configurations that yielded the highest resolution with complete UV coverage for polar sources. The configuration diameter versus the symmetry order is plotted in fig. 6. The array resolution increases as the symmetry order decreases because the sector length increasing faster than linearly with the number of antennas in each sector as shown in fig. 2.

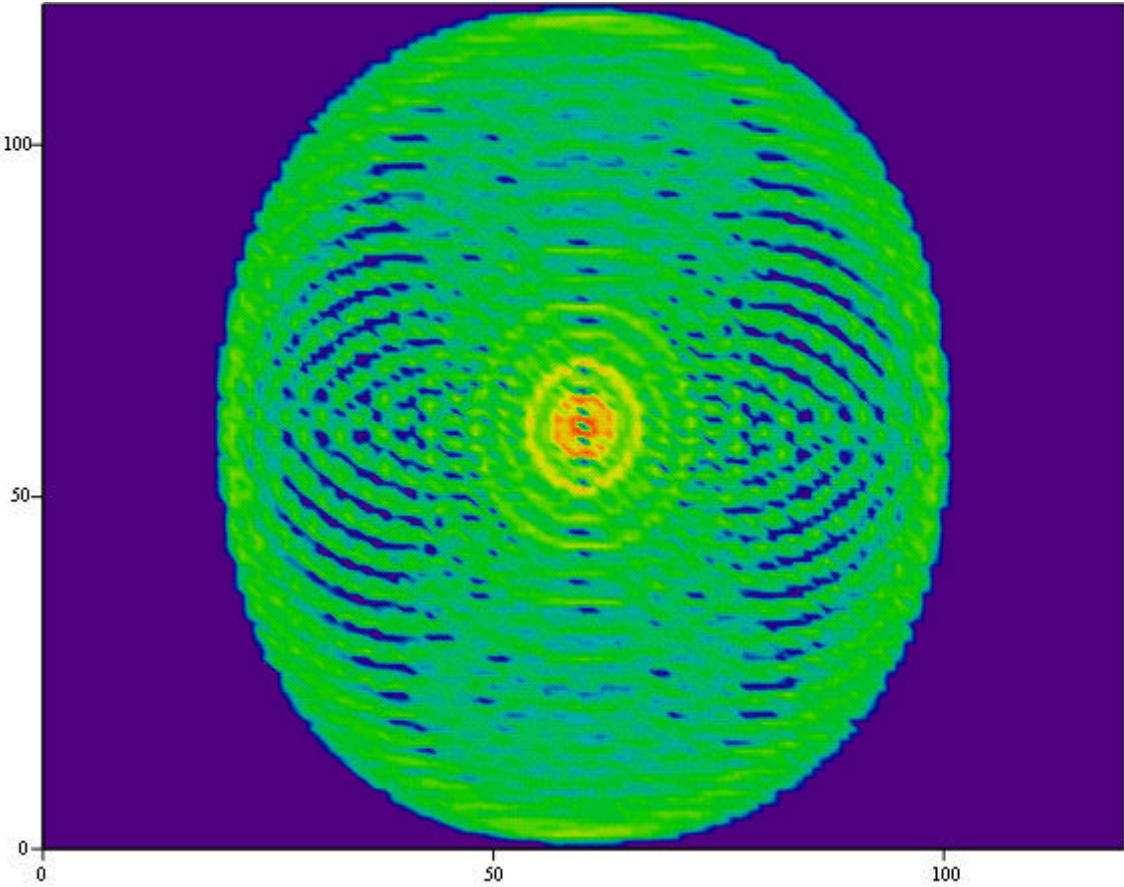


Fig. 7 UV coverage for an elliptical array with 21 sectors and 3 antennas in each sector. The source is at  $-10^{\circ}$  DEC and was tracked for two hours through transit.

The S-fold symmetric circular array configuration is only guaranteed to give complete UV coverage with earth rotation for polar sources and a configuration that projects to a circle for these sources. Sources at other declinations require explicit calculations to evaluate the coverage as a function of hour angle range. The configurations listed in Table 1 were elongated by a factor of 1.5 in the north-south direction and placed at  $-23^{\circ}$  latitude to simulate possible ALMA arrays. An example of the signal-to-noise across the UV-plane for a two hour (+1 hour of transit) observation of a source at  $-10^{\circ}$  DEC using the 21 sector 3 antennas per sector configuration is shown in fig. 7.

Figure 8 shows the hour angle range required to achieve 90% UV coverage for the configurations listed in Table I. Figure 9 shows the hour angle range required for 98% coverage. These plots show how the angular resolution can be traded off against the time required to obtain a given UV coverage. The plots also show the difficulty of using earth rotation to fill in the UV-plane for equatorial sources. Even so, reasonable coverage for all declinations can be obtained using one configuration and simply extending the observing time for the equatorial sources.

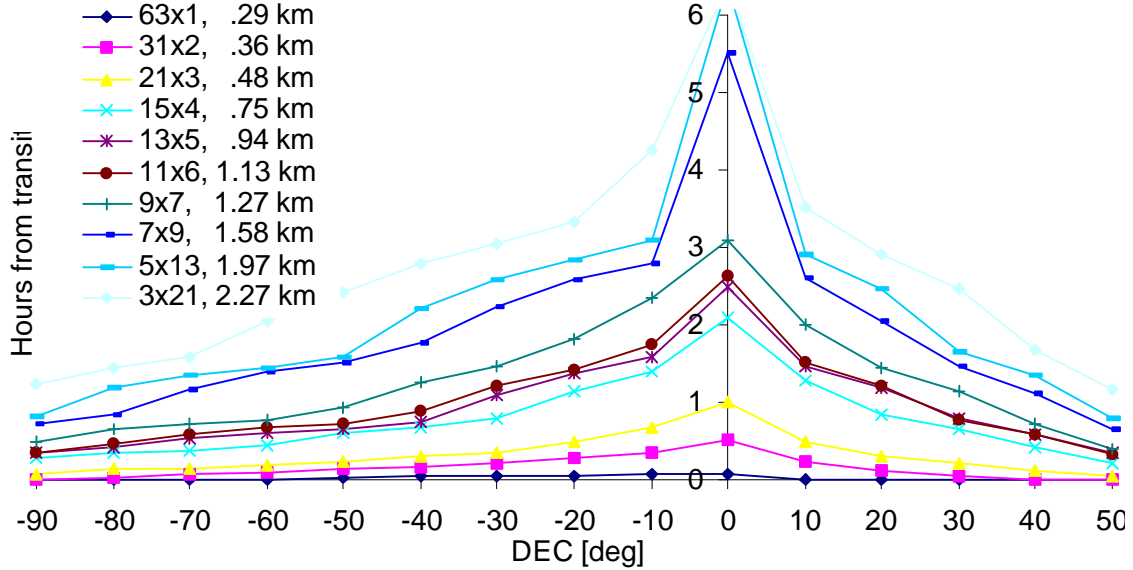


Fig. 8. Hours before and after transit required to achieve 90% UV coverage as a function of source declination for the configurations given in Table I.

#### IV. Mosaicing and shadowing

Mosaicing will be an important component in the ALMA observing program. We can distinguish between two types of mosaic observations. The easiest will be “wide-field surveys” for small objects over fields wider than the primary beam. “Wide-field mapping” of the emission from structures larger than the primary beam will be more difficult.

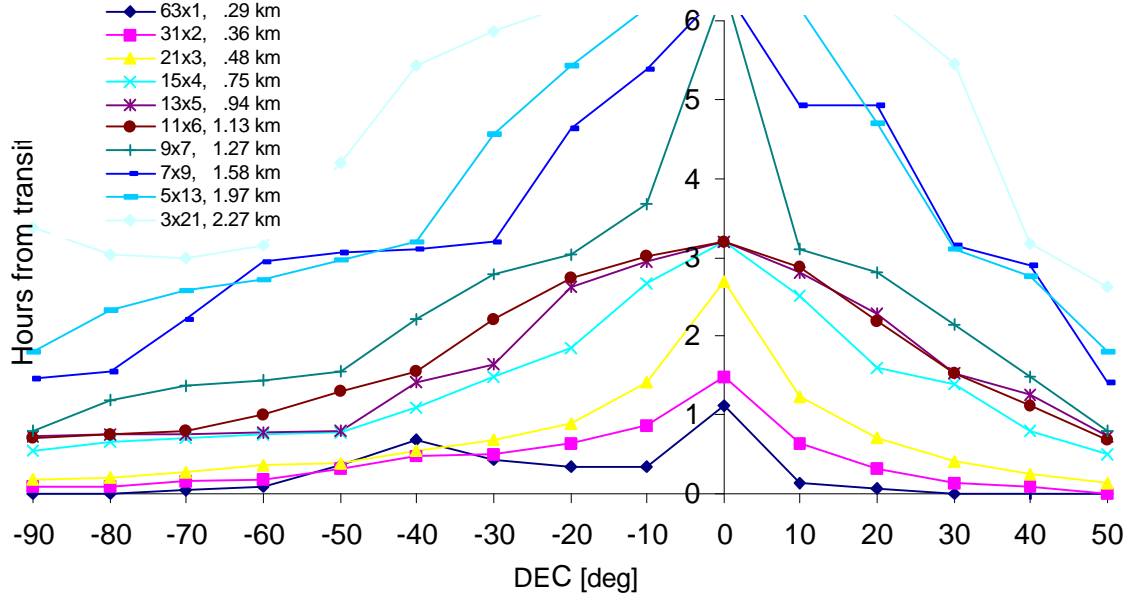


Fig. 9 Hours before and after transit required to achieve 98% UV coverage as a function of source declination for the configurations given in Table I.

Wide-field surveys will require multiple pointings, but the images from each field can be processed independently and combined by mosaicing the images together in the final step. It is only necessary to have the long baselines corresponding to the scale size of the survey objects of interest and complete UV coverage is not required.

On the other hand, wide-field mapping requires obtaining the visibilities in the UV-plane with a resolution smaller than the single pointing UV resolution spot. This is accomplished using multiple pointings as in the wide-field survey mode but the data are usually processed together as a complete data set. Faithful images on all scale sizes require nearly complete UV coverage. Basically, the information content is directly related to the UV coverage. It makes little sense to obtain the visibility on a fine scale over part of the UV-plane and then leave large gaps in the UV coverage.

The overall flux level across a wide-field is often required so that the total emission and molecular mass can be determined. This is known as the “short-spacing” problem since it is the visibilities near the center of the UV-plane that measures this widely distributed emission. Single-dish observations measure the visibilities within  $\sim D/2$  of the center of the UV-plane while a pair of touching telescopes can yield reliable visibilities as close as  $\sim D/2$  from the center of the UV-plane. Even in this theoretical situation the signal-to-noise is reduced by a factor of two at the  $D/2$  ring as can be seen from the UV responsivity plotted in fig. 1. Ironically it is easier to obtain fine scale UV data at the longer baselines where different pairs of telescopes and earth rotation allows the high sensitivity center of the UV response function to be moved almost continuously across the UV-plane.

The existing sparse millimeter arrays have found that it is difficult to obtain the necessary short-spacing data and often resort to using single-dish data from telescopes two to three times larger than the array telescopes. One of the problems with a sparse array is that it is difficult to obtain close antenna spacings at all baseline orientations. The short spacings are acquired as the telescopes approach shadowing. This gives short observations at a few points around the center of the UV-plane. The five-fold symmetric 13 antennas per sector configuration in Table I has ten pairs of antennas with a separation of 1.2 D which gives 20 points around the center of the UV-plane, when the Hermitian property of the visibilities is taken into account. Figure 10 shows the instantaneous central coverage of the UV-plane for this configuration observing a source at  $-90^\circ$  DEC. The coverage is very dense and significantly better than any existing array. This should allow recovery of all of the short-spacing UV data using the array telescopes for the single-dish observations.

(An alternate approach to filling the short-spacing ring in the UV-plane is to build a dedicated array of five or six smaller telescopes that would be arranged to measure just the short-spacing visibilities. This concept arose out of discussions at Imaging99 and offers a less expensive option to building a single much larger telescope.)

Shadowing is an important constraint on array observations. Shadowing will corrupt the baseline between a telescope and the one in front of it casting the shadow, and will distort the beam and possibly cause problems on all baselines involving the shadowed telescope. For these reasons it is important to have configurations which provide the short-spacing data with a minimum of shadowing. The 1.2 D minimum

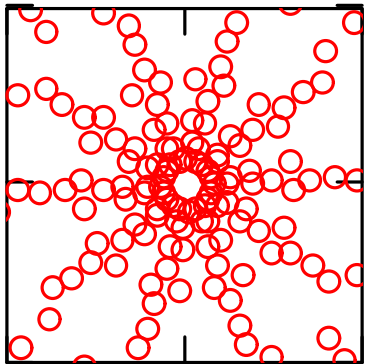


Figure 10. Inner 200 m of instantaneous UV coverage for 5x13 array configuration. The circles are 12 m in diameter and represent the area of the UV plane that can be reliably recovered using mosaicing techniques.

spacing used here is very aggressive, but there is at least one telescope concept that can operate safely at this spacing [Woody and Lamb, 1999]. The nominal 1.2 D spacing together with the 1.5 North-South elongation allows the 5x13 configuration to observe equatorial sources for ~4 hours around transit or transiting sources from  $-79^{\circ}$  to  $+33^{\circ}$  DEC without shadowing. The configuration can be modified to provide longer shadow free coverage and better short-spacing coverage for equatorial sources by moving just ten telescopes a few meters. These same ten telescopes can be moved in the opposite direction to improve the short-spacing coverage and shadowing for sources at the extremes of the declination range. It would be sensible to have two possible stations for these ten critical telescopes to optimize the configuration for the two declination ranges. It should only take one day to move these ten telescopes.

## V. Discussion

Imaging techniques and array configuration evaluation is different for configurations that achieve nearly complete UV coverage. The problem changes from one of producing models that give the best fit to sparse UV data without “over interpreting” the data to the problem of minimizing the artifacts resulting from missing a small percentage of the data. This later problem is the usual situation for many groups working on image reconstruction in fields such as medical imaging or synthetic aperture radar. These groups use instruments designed to provide complete images except that a small percentage of the data is missing due to noise or hardware failure.

The measured visibilities will fill all but a few of the UV-cells for a map of a single small field. The small gaps in the visibility data can to first order be filled by interpolation from the neighboring UV-cells. Accurate images can then be obtained by simple Fourier transformation. The beam for a fully sampled disk in the UV-plane is simply the usual Airy pattern and the sidelobes can be reduced by applying Hanning or similar weighting to the visibility data. “Clean” algorithms can also be applied to the few brightest sources to minimize the Airy pattern sidelobes from these sources for high dynamic range images. In contrast to most “cleaned” images with sparse UV coverage, the residuals after removing the cleaned components from nearly complete UV coverage maps will contain accurate image information.

The noise across the UV-plane will vary with the total integration time for the data in each UV-cell. Hence, the detection limit will depend upon the scale size of the structure in the image plane. The typical signal-to-noise distribution shown in fig. 5 for circular arrays gives better detection limits for the smallest and largest objects than for intermediate scale size objects. It can be argued that many observations would benefit from this distribution in sensitivity. Sharp high-resolution images are produced that also yield sensitive measurements of the integrated flux across the field.

A possible suite of configurations for ALMA is:

- 1) Compact configuration with all of the antennas in a 150 m diameter hexagonal closed packed disk for optimum surface brightness sensitivity
- 2) Uniform 300 m diameter circular array for fast complete snapshot images.
- 3) 11-fold symmetric 1 km diameter circular array for quick complete images at all declinations at modest resolution (.2 arcsec at 1mm).
- 4) 5-fold symmetric 2 km E-W x 3 km N-S elliptical array for high resolution images (.1 arcsec at 1mm) and complete images for 2 to 8 hour long observations
- 5) 10 km diameter circular array for ultra-high resolution mapping.

## VI. Summary and Conclusion

This study shows that ALMA can produce tenth arcsec complete images at 1 mm for all declinations using a single five-fold symmetric elliptical configuration. Other configurations, such as the Keto type rings, can probably be found that produce complete images at even higher resolution, or in shorter time, or that work better for equatorial sources. This approach offers a solution to the problem of producing accurate (high dynamic range and high fidelity images) without making any assumptions about the source structure and with resolution equal to or better than the Hubble telescope.

## References

- Bock et al., MMA Memo 225, 1999.  
Carilli, C. L., and Holdaway, M. A., MMA Memo 262, 1999.  
Conway, J. E., MMA Memo 260, 1999.  
Keto, E., Ap. J., vol. 475, p. 843, 1997.  
Kogan, L., MMA Memo 247, 1999 plus others in this series.  
Woody, D. and Lamb, J., MMA Memo, 241, 1999.